Wireless Communication Technologies in Omnidirectional CubeSat Crosslink: Feasibility Study and Performance Analysis

Imam Uz Zaman, Ahmed Eltawil, *Senior Member, IEEE*, and Ozdal Boyraz

***Abstract*—An efficient omnidirectional CubeSat data crosslink is imperative to ensure the success of resource-intensive advanced CubeSat missions. In this article, we present a feasibility study of wireless technologies in high-speed CubeSat crosslink design. We study the power consumption, pointing requirement, and antenna requirement of each technology to implement an omnidirectional communicator. We also investigate the performance limit of the state-of-the-art wireless technologies considering the realizable link parameters. The achievable data rate and communication distance are studied thoroughly for different communication systems. The analyses show that an optical communication link is capable of delivering more than two orders of magnitude higher data throughput than that of microwave links in an omnidirectional platform. However, the study shows that due to the size and power restriction, a performance crossover region exists where the performance of a microwave channel exceeds the performance of the optical channel. The crossover distance and crossover data rate are studied thoroughly with different system configurations and modulation formats to assess the maximum reach of wireless technologies in a CubeSat crosslink.**

***Index Terms*—Crosslink, CubeSat, omnidirectional link, optical communication, radio frequency (RF), small satellite, wireless communication.**

I. Introduction

OVER the years, CubeSats have evolved from purely educational tools to a prevailing platform for technology demonstration and scientific instrumentation [1]–[3]. Advanced CubeSat missions must be designed in such a way that each one of the CubeSats in a constellation is assigned to a specific time-synchronous role, and collaboratively, they are missioned to accomplish a complex task [4]–[6]. The 3-D CubeSat constellations in the space as shown in Fig. 1 necessitate a high-speed data communication with about 360° field of regard (FOR) to enable point-to-point data communications as well as data relaying among an arbitrary set of satellites simultaneously [7]. Therefore, the realization of the omnidirectional intersatellite link is important to ensure the success of such constellation-based missions. A CubeSat is a type of nanosatellite that is constructed in modules of multiples units (U), 1 U $\approx 10\times10\times10$ cm^3. Typical weight of a 1U CubeSat is about 1.33 kg and the available average power with the nondeployable solar panel is less than 2.5 W/U [8]–[10]. Size, weight, and power-cost (SWaP-C) have never become so crucial as it is in the typical CubeSat platforms (smaller than 12U [11]) where the performance metrics clash with the available volume (less than $23\times24\times36$ cm$^3\approx$ 0.02 m^3), weight (less than 16.3 kg), and available payload power around 50 W with deployable solar panels that can generate up to 130 W power [12], [13]. Therefore, the successful implementation of the omnidirectional communication necessitates a detailed analysis of the strengths and weaknesses of the wireless technologies considering the distinct physical and technological constraints imposed by the CubeSat technology. Microwave [radio frequency (RF) and millimeter wave (mmWave)] and optical communication offer different benefits and challenges to enable omnidirectional communication in such a platform.

Recent progress in the RF and mmWave demonstrate high data rates (up to 1.6 Gb/s) point-to-point communication with complex subcarrier modulations and high-power consumption [14], [15]. The adaptable deployment of such microwave systems for simultaneous communication among multiple satellites in a constellation is constrained by the bandwidth restriction, the available power, and the required antenna gain. Optical communication technologies have excellent directivity, and therefore can achieve higher data rates with much smaller antenna size and power consumption [16]–[18]. Nevertheless, the implementation of a pointing, acquisition, and tracking (PAT) system in an optical communication system is a challenging task [19]–[21]. The achievability of the stringent pointing accuracy is well studied and demonstrated with advanced PAT systems and careful optical designs [20], [22]–[24]. For instance, one of the most recent CubeSat missions, CLICK, presents the feasibility of achieving ±0.45 millidegrees pointing accuracy that can maintain a 20-Mb/s data rate at a range over 580 km [20]. The required single-axis pointing

Manuscript received January 5, 2021; revised April 25, 2021; accepted May 3, 2021. Date of publication May 11, 2021; date of current version August 23, 2021. This work was supported in part by the Office of Naval Research under Grant N00014-18-1-2845. *(Corresponding author: Imam Uz Zaman.)*

The authors are with the Department of Electrical Engineering and Computer Science, University of California at Irvine, Irvine, CA 92617 USA (e-mail: zamani@uci.edu; aeltawil@uci.edu; oboyraz@uci.edu).

Digital Object Identifier 10.1109/JMASS.2021.3079102

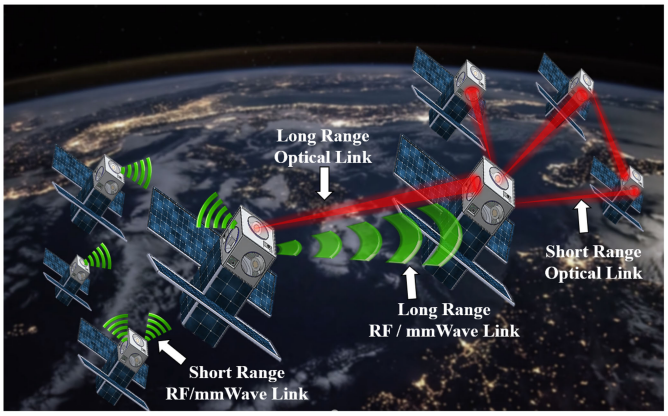

Fig. 1. Wireless communication systems for CubeSat crosslink. RF, mmWave, and optical communication are the promising modes of omnidirectional communication in both short and long range.

requirement of the CLICK mission is about ±1.4 millidegrees [20]. Recent advances in star tracking technologies, as well as scanning mirror technologies, demonstrate better than 0.28 millidegrees pointing accuracy [22], [25], [26]. With the ongoing advancement of the PAT sensors and scanning mirror technologies, we believe the pointing accuracy requirement of the optical communication can be addressed. Most of the earlier efforts in CubeSat communication spent on the performance optimization of a point-to-point communication link. The feasibility study of the wireless technologies in omnidirectional communication (one to many nodes) along with a detail comparative study of the performance reach of the technologies are still open for investigation.

In this article, we present an in-depth feasibility study and performance analysis of the available wireless technologies for the omnidirectional CubeSat platform. We show that there is a crossover distance below which optical communication outperforms microwave technologies, and beyond the crossover distance, microwave technologies offer higher bit rates due to their inherent low-receiver (Rx) sensitivity. In particular, we study and compare the performance of RF (2.4, 5, and 26 GHz), mmWave (34 and 60 GHz), and optical communication (from 180 to 400 THz) medium with self-imposed boundary conditions to satisfy the CubeSat SWaP-C constraints. We investigate the realizable data rate in different simple modulation formats with realistic physical constraints. We calculate the crossover distance and crossover data rate of different system combinations and modulation formats to identify the maximum reach and the maximum data rate of the communication systems. Furthermore, we study the feasibility of wireless technologies in achieving omnidirectionality in terms of power consumption and antenna requirements.

II. Comparative Study of the Link Budget Parameters

The comparative performance study of the wireless communication begins with the well-known link budget equation that estimates the received power P_{rcv} based on the transmitted power P_T, total antenna gain G, total loss L, and combined antenna efficiencies η in a simple formula that is expressed as $P_{\text{rcv}} = P_T\ G\ L\ \eta$. Total antenna gain G here is the combined gain of the transmitter (Tx) antenna gain $G_T = f(D_T, \lambda)$ and Rx antenna gain $G_R = f(D_R, \lambda)$, i.e., $G = G_T G_R$. Here, D_T, D_R, and λ represent the Tx diameter, Rx diameter, and operating wavelength, respectively. Total loss L includes Tx feeder loss L_{Tx}, Rx plumbing loss L_{Rx}, the path loss L_R, and the pointing loss $L_P = f(G_T)$ and, therefore, L can be expressed as $L = L_{\text{Tx}} L_{\text{Rx}} L_R L_P$. Assuming that we have Tx and Rx antenna efficiencies of η_T and η_R, respectively, we define the combined antenna efficiency as $\eta = \eta_T \eta_R$. Almost all of these parameters depend on the antenna sizes, available electrical power, and wavelength. Hence, constraints imposed by CubeSat dimensions differ significantly from the constraints imposed by relatively large satellites despite the fact that the performance expectations are quite similar. Hence, we impose several boundary conditions pertinent to the CubeSats platform. Some of these self-imposed conditions are: 1) CubeSats are smaller than 12U [11]; 2) total power consumption of the communication payload is less than 50 W (12U limit) [13], [27]; 3) microwave antenna size (dish size) is less than 200 mm; 4) maximum optics diameter is 50 mm (due to weight limitation) [27]; 5) $P_T = 1$ W; and 6) antennas are nondeployable to accommodate multiple antennas to achieve omnidirectionality.

The major distance-dependent loss parameter in the above link budget is the path loss $L_R = f(f, r)$ that depends on the carrier frequency f and distance r. The path loss L_R between the feed points of two isotropic antennas in free space at a distance r can be given as $L_R = (c/[4\pi fr])^2$. Here, f and c are the carrier frequency and the speed of light, respectively. Due to higher carrier frequency, the optical communication experiences a higher path loss (more than 50 dB) compared to that of the RF and the mmWave frequencies. However, this large path loss at optical frequencies is usually compensated by the high antenna gains (i.e., Tx and Rx gains) in the link budget equation.

The transmit antenna gain G_T represents the power transmitted by an antenna in a specific direction as compared to an isotropic antenna and can be estimated from the full-divergence angle (θ) [in rad] of the transmit beam $G_T \approx (16/\theta^2)$ [28], [29]. Since, $\theta = f(\lambda, D_T)$, the G_T can also be estimated as $G_T \approx ([\pi\ D_T]/\lambda)^2$. The Rx antenna gain G_R is defined as the ratio of the powers received by the Rx antenna and an isotropic antenna, and it can be defined as $G_R \approx (\pi\ D_R/\lambda)^2$. It can be realized that both G_T and G_R are proportional to the square of the diameter to the wavelength ratio (D_k/λ) where $k \in \{T, R\}$. Here, T and R represent the Tx and the Rx, respectively. In other words, the larger the antenna diameter, the higher is the gain. In contrast, smaller wavelengths (or higher carrier frequencies) realize higher antenna gains for a given antenna dimension. Consequently, optical frequencies possess a much larger antenna gain as compared to RF and mmWave systems for a given antenna size. The upper limit of the antenna size is limited by the available volume, size, and weight of the CubeSat platform. The RF and mmWave communication systems usually use the same physical antenna to send and receive the signals, therefore, $G_T = G_R$. On the contrary, most of the optical transceivers

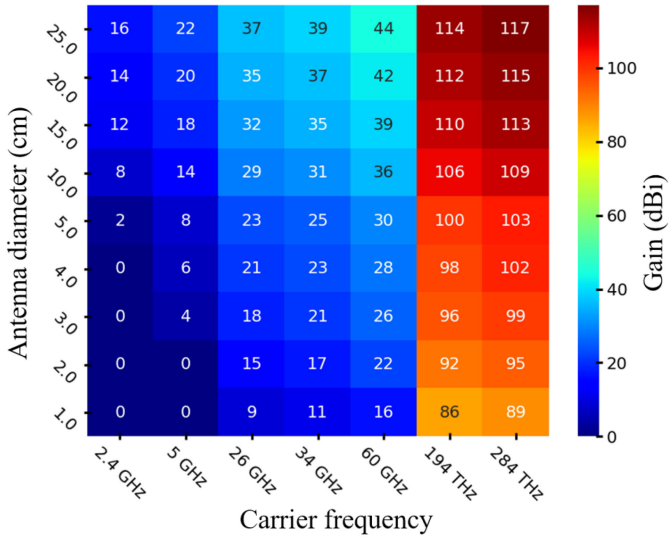

(a)

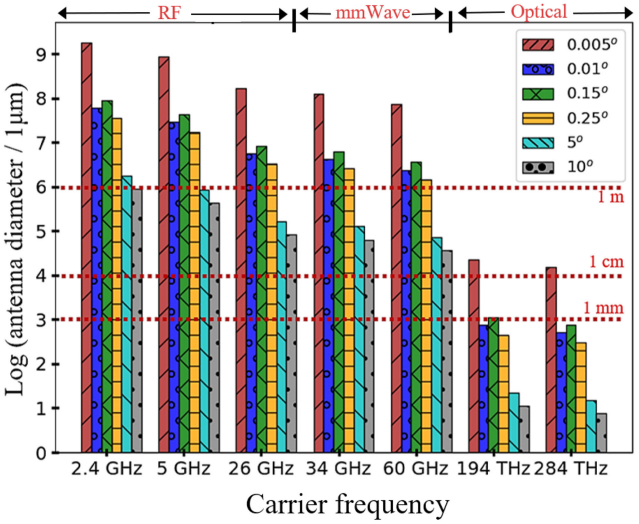

(b)

Fig. 2. (a) Achievable antenna gain for different carrier frequencies (*x*-axis) and antenna diameters (*y*-axis). (b) Required antenna diameters for different full divergence angles.

incorporate Txs with smaller optics (D_T) and the Rx with comparably larger optics (D_R). Therefore, the antenna gains G_T and G_R can be very different in optical communication. The achievable gains (either G_T or G_R) for different antenna sizes and carrier frequencies are presented in Fig. 2(a). It can be seen from Fig. 2(a) that microwave systems can achieve a total gain of about 84 dBi ($G_T + G_R \approx 42$ dBi+42 dBi) by using a 20-cm antenna diameter. In contrast, more than 100 dBi antenna gain is readily achievable in optical frequencies by using optics that are more than five times smaller in dimension than that of microwave antennas. For instance, a combined antenna gain of about 182 dBi ($G_T + G_R \approx 86$ dBi+96 dBi) is achievable with a 10 mm Tx beam and a 30 mm Rx aperture at 194-THz (1550 nmβ wavelength) optical communication system. The feature that leads to the high antenna gain is the high antenna directivity (small beam divergence angle θ). The diffraction-limited full-beam divergence angle θ [in degrees] can be estimated as $\theta \approx 1.26([180\lambda]/[\pi D_T])$ [30], [31]. The estimation of θ is applicable to directive antennas. In directive antennas, the antenna diameter is larger than the communication wavelength, i.e., $D_T > \lambda$. The required antenna diameters (normalized to 1 μm) to achieve different θ is shown in Fig. 2(b). For instance, it can be seen that 60, 5.55, 2.4, and 0.74 mm antennas are required for 2.4 GHz, 26 GHz, 60 GHz, and 194 THz carrier frequencies, respectively, to achieve a beam divergence of about 0.15°. It is evident that a small divergence angle (less than 1°) is not feasible in RF and mmWave communication systems due to the need for a very large antenna diameter that exceeds commonly used CubeSats (1U–12U) dimensions. However, optical antennas can achieve a very small divergence angle (less than 0.01°) with less than 1-cm antenna (i.e., telescope) aperture.

Although high directivity is desired for an efficient power delivery to the Rx antenna, it comes with a stringent pointing accuracy requirement. Therefore, a sophisticated pointing and acquisition system needs to be implemented to maintain effective data transfer in the optical communication system [17], [19], [20]. To achieve a throughput loss of less than 3.0 dB, the required pointing accuracy ϵ (in degrees) of an intersatellite communication should be as small as $\epsilon \approx ([180\lambda]/[20\pi D_T])$ [29]. The required pointing accuracy for different antenna sizes and operating wavelengths is calculated and presented in Fig. 3. It can be seen from Fig. 3 that about 57°–0.07° pointing accuracy is needed for RF frequencies (up to 25 GHz) with the antenna diameter ranges from 1 to 50 cm. The mmWave link, the frequency range of 26 to 300 GHz, requires about ten times higher pointing accuracy (approximately 5.5°–0.007°) compared to RF for the same antenna diameter range. Evidently, the optical regime has the most stringent pointing accuracy requirement of 0.5 millidegrees to 5.5 μdegrees for optical frequency greater than or equal to 180 THz for the same aperture sizes.

The required pointing angle in optical communication directly depends on the beam divergence of the transmit beam. The higher the beam divergence, the lesser the pointing accuracy is required. For instance, an optical communication between two stratospheric platforms that mimic two small satellites demonstrated a pointing requirement of less than 0.5° by transmitting a high diverging (0.4°) 808-nm signal [32].

There exist intertwined relationships among the above-mentioned link parameters. For example, a large transmit antenna gain G_T is achieved in mmWave and optical communication by transmitting a high directional beam (low θ). The high directional beam tends to cause a higher pointing loss L_P, and hence the beam pointing and tracking between the Tx and Rx becomes a challenging task [21], [33]. As described in the next section, the high directional beam also necessitates a larger number of Txs to attain the omnidirectionality (360° FOR). Moreover, it is apparent from the path-loss equation that optical communication experiences a higher loss compared to that of RF and mmWave due to higher f. The detailed communication link performance considering the interplay among all the link parameters is investigated in Section V.

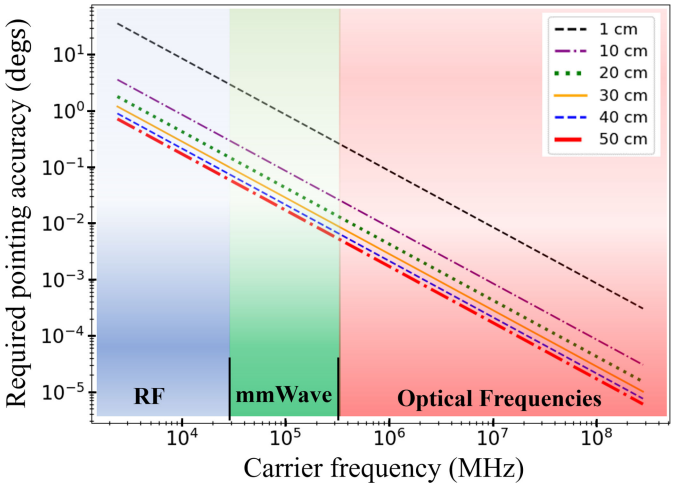

Fig. 3. Required pointing accuracy for different wireless links to achieve less than 3-dB throughput loss.

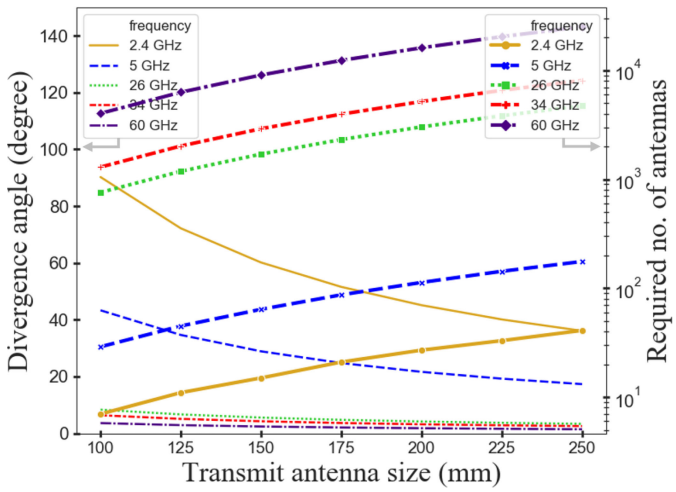

Fig. 4. Required number of transceivers to achieve a full FOR.

III. Transceiver Antenna Requirement for Omnidirectional Communication

To achieve an omnidirectional communication, both the Tx and the Rx need to possess a full FOR (360°). The required number of transceivers to achieve an FOR of α_{req} (in degrees) can be given as

$$n \approx \text{ceiling}\left(\left(\frac{\sin(\pi\alpha_{\text{req}}/720)}{\sin(\pi\alpha/720)}\right)^2\right). \quad (1)$$

Here, α is the FOR (in degrees) of a single transceiver system. In the case of directional RF and mmWave antenna (patch antenna and dish antenna), α corresponds to the antenna beamwidth (or divergence angle). In a phased array antenna (PAA)-based system with a full scanning angle of α_{PAA}, $\alpha = \alpha_{\text{PAA}}$. In a scanning mirror-based optical communication system with a full mechanical scanning range of α_{mec}, $\alpha \approx 2\alpha_{\text{mec}}$. The required number of transceivers needed to achieve omnidirectional communication in a static (nonbeam steering) RF and mmWave communication system is calculated from (1) and shown in Fig. 4. It can be seen from Fig. 4 that a 2.4 GHz RF system requires 15 and 27 antennas when the antenna diameters (size of the dish) are 150 and 200 mm, respectively. The requirements of a large number of antennas are a direct consequence of transmitting a high directional beam to achieve a large antenna gain. Moreover, a higher operating frequency demands for larger n. Therefore, realizing an omnidirectional high-speed and long-distance communication in RF and mmWave is extremely difficult with dish antennas or patch antennas due to the tradeoff among G_T, G_R, and n. Although nondirectional microwave antennas, such as dipole antennas, can achieve full FOR with fewer number of antennas, the communication range will be very limited due to low antenna gains. For instance, a single half-wave dipole antenna can act as an omnidirectional antenna but the antenna gain is about 2.4 dBi.

The emerging PAA enables effective beam switching and beam scanning in the RF and mmWave system and therefore, it possesses the potential to achieve a full FOR with a lesser number of transceiver units than the calculated n in Fig. 4. Many PAA systems have been demonstrated in the past several years. Recent progresses in the multielement (up to 64 elements) PAA with a frequency range of 26–30 GHz demonstrate the feasibility to achieve high gain (up to 40 dBi) and wide beam steering capability (more than ±50°) [34]–[37]. Based on the beam steering angle of the PAAs, using (1), we estimate that approximately 2, 19, 7, and 6 PAA antenna systems are required to achieve an omnidirectional communication for the antenna systems mentioned in [34]–[37], respectively. Since the state-of-the-art RF and mmWave PAA still possess a large beam divergence (usually greater than 5°), they demonstrate low antenna gains compared to the optical antennas [34]–[37]. The low antenna gain limits the attainable communication range. Besides, the state-of-the-art PAA systems are power-hungry systems, therefore, the implementation of the required number of antennas is limited by the available power in the SWaP-C limited CubeSat platform. On the other side, COTS high-speed (about 1 kHz) scanning mirror technologies are compact (diameter less than 15 mm) and they can achieve a wide optical scanning angle (as high as 100°) [38]. For this reason, it is possible to obtain a full FOR in a less than 6U CubeSat platform by incorporating 9 and 6 independent transceivers accompanied by scanning mirrors with full mechanical scanning ranges of 40° and 50°, respectively [3], [39].

IV. Sample Power Consumption Estimation of Wireless Transceivers

Power consumption is the most demanding subject in a CubeSat platform. We can assess the challenge with simplified sample block diagrams of a microwave transceiver (RF and mmWave) and an optical transceiver that is presented in Fig. 5(a) and (b), respectively. The short description of the components, the gain or loss values, and the approximate power consumption of the major link components are summarized in Table I. The power consumption of the passive components (PCs) is set to zero. The splicing and pump

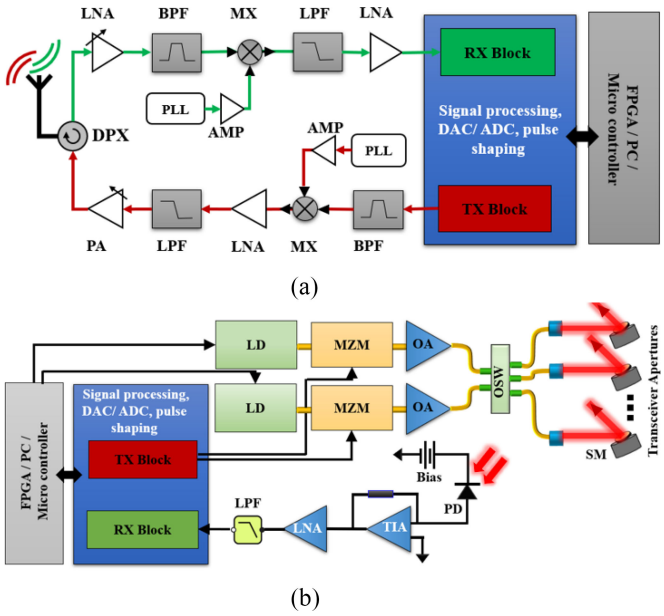

Fig. 5. Sample block diagrams of the transceiver architectures. (a) RF and mmWave. (b) Optical.

TABLE I
PARAMETERS OF THE MAJOR TRANSCEIVER COMPONENTS

Item	Description	Gain/Loss (dB)	P(W)
LNA	Low noise amplifier	$\approx +25$	≈ 0.3
BPF	Band pass filter	≈ -0.2	0.0 (PC)
LPF	Low pass filter	≈ -1.8	0.0 (PC)
MX	Mixer	≈ -9.0	0.0 (PC)
PA	Power amplifier	$\approx +24.5$	≈ 2.4
PLL	Phase locked loop	N/A	≈ 0.1
AMP	Amplifier	$\approx +13.0$	≈ 0.25
DPX	Duplexer	≈ -1.5	0.0 (PC)
LD	Laser diode (100 mW)	N/A	≈ 0.5
MZM	Mach-Zehnder modulator	≈ -5.0	≈ 0.25
OSW	Optical switch	≈ -0.8	≈ 0.2
TIA	Transimpedance amplifier	$\approx +32.5(k\Omega)$	≈ 0.3
OA	Optical amplifier	$\approx +15$	≈ 3.5
SM	Scanning mirror	≈ -0.15	≈ 0.5
SPC	Splicing and pump combiner	≈ -0.1	0.0 (PC)
TX Block	Tx signal processor	N/A	≈ 3.0
RX Block	Rx signal processor	N/A	≈ 2.5

combiner (SPC) losses of the optical transceiver are lumped together in the table and not shown in Fig. 5(b).

The sample power consumption approximation of the sample microwave communication link (RF and mmWave) is based on the manufacturer's specification of the COTS components [40]–[45] and state-of-the-art communication system models [7], [46]. We calculate the power consumption of a microwave Tx to produce a 1 W output power is about 6 W (using Table I). Similarly, the estimated Rx power consumption is about 3.45 W. Hence, to establish a point-to-point link with a 1-W transmit power, the microwave communication system requires at least 9.45 W of electrical power. The power consumption of the optical transceivers is dictated by the realizable efficiencies of the lasers and the optical amplifiers (OAs) that can vary quite a bit from one system to another. To estimate the power consumption, we consider a 1550-nm (194 THz) optical communication system. Besides, we assume the wall-plug efficiencies of the laser diode (LD) and OA are approximately 20% and 15%, respectively. At a 50% duty cycle about 500 mW average output optical power is required to generate a 1 W peak optical power. As shown in Fig. 5(b), about 16 dB optical gain is needed from OA to achieve a 1 W peak power that incorporates a 100-mW LD. Therefore, considering the data provided in Table I, the optical Tx power consumption, $P_{\text{TXOPT}} \approx 8.0$ W, and the Rx power consumption, $P_{\text{RXOPT}} \approx 3.0$ W. Therefore, the sample optical transceiver consumes at least 11.0 W of electrical power. The transceiver power consumption depends on the system design and component selection. The approximate power calculation is provided here to provide the readers with a comparative idea of the power requirements of microwave and optical links.

Despite such high-power requirements from transceivers, SWaP-C restrained CubeSat solar panels can provide a limited amount of energy from a single source: Sun. For example, if we consider a system with commercially available components, state-of-the-art high-end solar panels, such as eHawk [16], can generate about 75–140 Wh averaged electrical power in 6U to 12U platforms, respectively. Assuming that only 40% of the total power is allocated for a continuous communication payload, the available average power is about 30–56 Wh in 6U to 12U CubeSat platforms. Omnidirectional communication can be feasible in S-band and C-band systems with monopoles or 2–4 patch antennas, but with a limited range depending on the available bandwidth and the modulation formats. However, incorporating multiple active PAA to facilitate the beam steering-based omnidirectional communication is challenging with the existing PAA due to the high-power consumption, e.g., greater than 500 W for a single 64 element system [47]. In contrast, the advancement in miniature high scanning speed mirror technologies (power consumption less than 0.5 W) such as microelectromechanical systems (MEMS), dual-axis vector mirror-based optical transceiver can achieve a full FOR with a predefined number of transceivers and reasonable power consumption as described above. For instance, in the example design shown in Fig. 5(b), it can be estimated that about 16.5 W electrical power is required to operate two simultaneous optical communication links (one point to point and one data relaying). The detailed design challenges and tradeoffs of the omnidirectional optical transceivers were presented in [3] and [48].

V. COMPARATIVE PERFORMANCE ANALYSIS

We study the achievable data rate and the communication distances of wireless point-to-point communication systems with different modulation formats and design parameters. The RF, mmWave, and optical links are quite different from each other when considering the realistic link parameters. To analyze the communication performance, we consider the values of each parameter based on the state-of-the-art systems in

TABLE II
LINK BUDGET PARAMETERS

Parameter	Wireless technologies	Value
Transmit power (P_T)	RF, mmWave, optical	1 W
Tx diameter (D_T)	RF, mmWave	5 to 20 cm
	Optical	10 mm
Rx diameter (D_R)	RF, mmWave	5 to 20 cm
	Optical	50 mm
Pointing loss (L_P)	RF	-0.3 dB
	mmWave	-1.0 dB
	optical	-3.0 dB
Tx-Rx feeder loss	RF	-5.1 dB
	mmWave	-4.1 dB
	optical	-3.5 dB
Receiver sensitivity	RF, mmWave	≈-108 dBW
	optical	≈-90 dBW
Receiver noise figure	RF,mmWave	6 dB
Photodiode gain	optical	100
Noise equivalent power	optical	$30\,pW/\sqrt{Hz}$
Photodiode bandwidth	optical	1 GHz
Link margin (M)	RF, mmWave, optical	-3 dB

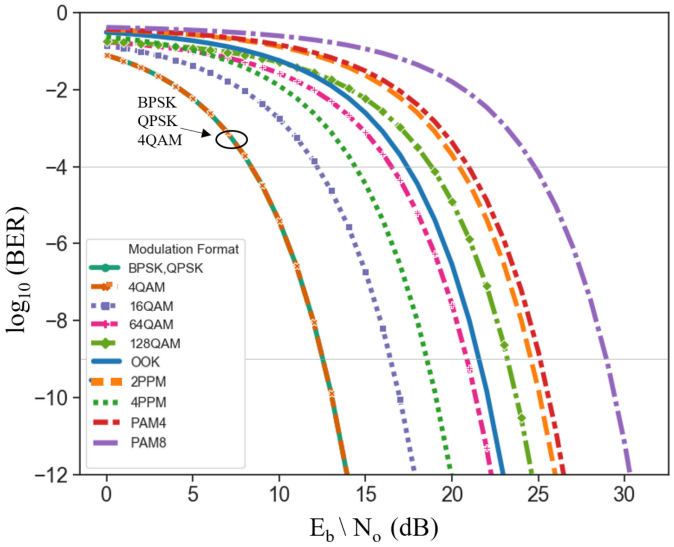

Fig. 6. BER versus E_b/N_o for different modulation formats.

literature and manufacturer specifications. For example, the microwave link parameters alongside link performances are analyzed in [17] and [49]–[52]. Similarly, potential omnidirectional optical link parameters are mentioned in [7], [24], and [49]. Considering the CubeSat SWaP-C constraints and the size of optics (volume and weight), the sample optical system incorporates optical Tx aperture, $D_{T(\text{opt})} = 10$ mm and Rx aperture, $D_{R(\text{opt})} = 50$ mm. Since RF and mmWave antennas are relatively lightweight and compact, we consider three different antenna sizes, $D_{k(rf,\text{mmWave})} = \{100$ mm, 150 mm, 200 mm$\}$. Here, the subscript $k \in \{T, R\}$, where T and R represent the Tx and the Rx, respectively. The remaining link parameters considered in our analyses are summarized in Table II.

A. Achievable Data Rate in Different Modulation Formats

Assuming antenna efficiencies, $\eta_T = \eta_R = 1$, the link budget equation stated in Section II can be simplified in terms of physical link parameters to estimate the power at the Rx P_{rcv} (in dB)

$$P_{\text{rcv}} = P_T + 20\log(R_T) + 20\log(R_R) - 20\log(r) - 20\log(\lambda) + 10\log(L_P L_R L_T) + 9.943. \quad (2)$$

Digital communication systems require a certain ratio of energy per bit E_b to noise density N_o ($N_o = [N/B]$), E_b/N_o. Here, N is the total noise power and B is the communication bandwidth. The required received power P_{req} to realize a target data rate R_b can be expressed as $(P_{\text{req}}/N) \approx (E_b/N_o) \times (R_b/B) \times M$. The R_b (in dB) can be approximated as $R_b \approx (P_{\text{req}}/N) - (E_b/N_o) + B - M$. If the available received power is more than the required power, i.e., $P_{\text{rcv}} > P_{\text{req}}$, the communication link is overpowered and may waste energy. The R_b in this case is limited by the bandwidth of the Rx system. On the other hand, if $P_{\text{rcv}} < P_{\text{req}}$, the communication link cannot support error-free data communication at the target R_b.

To establish an error-free data communication, the state-of-the-art forward error correction (FEC) schemes, such as Turbo codes, convolutional-RS codes (recommended by the Consultative Committee for Space Data System, CCSDS), or LDPC codes, require pre-FEC bit error ratio (BER) in the order of 10^{-3} to attain a post-FEC BER less than 5×10^{-15} [53], [54]. The pre-FEC BER estimation based on the required (E_b/N_o) for different modulation schemes, such as quadrature phase-shift keying (QPSK), binary phase-shift keying (BPSK), quadrature amplitude modulation (K-QAM), on–off keying (OOK), pulse position modulation (N-PPM), and pulse amplitude modulation (PAM-K), are summarized in (3) [55]–[57]. Here, K represent the level of QAM and PAM modulations. N represent the level of PPM modulation.

$$\begin{aligned}
\text{BER}_{\text{QPSK,BPSK}} &\approx \frac{1}{2} erfc\left(\sqrt{\frac{E_b}{N_o}}\right) \\
\text{BER}_{\text{K-QAM}} &\approx \frac{\sqrt{K}-1}{\sqrt{K}\log_2 K}\text{erfc}\left(\sqrt{\frac{3\log_2 K}{2(K-1)}\cdot\frac{E_b}{N_o}}\right) \\
\text{BER}_{\text{OOK}} &\approx \frac{1}{2}\cdot\text{erfc}\left(\frac{1}{\sqrt{2}}\cdot\sqrt{\frac{E_b}{N_o}}\right) \\
\text{BER}_{\text{N-PPM}} &\approx \frac{1}{2}\text{erfc}\left(\frac{1}{4}\cdot\log_2 N\cdot\sqrt{\frac{E_b}{N_o}}\right) \\
\text{BER}_{\text{PAM-K}} &\approx \frac{1}{2}\text{erfc}\left(\frac{1}{2\sqrt{2}}\cdot\frac{\log_2 K}{K-1}\cdot\sqrt{\frac{E_b}{N_o}}\right).
\end{aligned} \quad (3)$$

The above-mentioned mathematical expressions assume that the symbol energy is divided equally among all the bits, and the Gray encoding is used so that at acceptable SNR, one symbol error is correlated to exactly one bit error. The theoretically obtainable BER in different modulation formats at different E_b/N_o (in dB) is calculated and presented in Fig. 6. For instance, we can see that BPSK, QPSK, and 4 QAM modulations, all require a minimum E_b/N_o of around 12.5 and 8.5 dB to possess BER $\leq 10^{-9}$ and BER $\leq 10^{-4}$, respectively. In contrast, the PAM-4 and the PAM-8 modulations require very high E_b/N_o (more than 25 dB) to maintain BER $\leq 10^{-9}$.

In space communication, PAM-K and K-QAM ($K \geq 16$) are not usually used as they require linear amplifiers and the E_b/N_o requirement is significantly high (as shown in Fig. 6). Therefore, only suitable modulation schemes with low E_b/N_o are selected, as normally in the space environment, the link margin is very tight [53]. We also calculate the R_b that maintains a BER $\leq 10^{-9}$ for different carrier frequencies, modulation schemes, and microwave antenna sizes. The sample achievable data rates for OOK, 4-QAM, and 2-PPM modulation schemes are presented in Fig. 7. In this example, a 150 mm antenna size is considered for RF and mmWave systems, whereas the optical transceiver incorporates a 10 mm Tx aperture and a 50 mm Rx aperture. It can be seen that optical communication achieves $R_b \geq 1$ Gb/s up to around 200-km communication distance that is about 1–2 orders of magnitude higher than that of mmWave communication. Low-frequency RF channels (2.4 and 5 GHz) achieve $R_b \leq 1$ Mb/s when communication distance, $r \geq 100$ km. One can notice that in shorter distance (less than about 100 km), the optical communication system is overpowered for the given modulation formats. In other words, the theoretical achievable data rate (calculated from P_{rcv}) is much higher than the practical realizable data rate that is limited by the Rx bandwidth. Therefore, in shorter distance, the optical communication systems can provide tens of gigabits data rate if the Rx system is designed accordingly. At very long distances ($r \geq 400$ km), the achievable data rate of mmWave channels, as well as high-frequency RF communications (e.g., 26 GHz) exceed the estimated data rate of the optical communication. Therefore, there exists a performance crossover region between the optical system and the microwave system for given system parameters, e.g., antenna sizes, optics, transmit power, Rx design, etc.

The inherent low Rx noise of the microwave commnication system is one of the major advantages that facilitates longer communication distance at low data rates, which is the main reason for the performance crossover. For instance, Fig. 8 shows the achievable R_b at $r = 500$ km. The system parameters used in Fig. 8 are the same as used in Fig. 7 that uses $D_{k(rf,\text{mmWave})} = 150$ mm. It can be seen that a 60-GHz communication system with a 150-mm antenna can theoretically achieve an R_b of about 30 Mb/s in a BPSK modulation that is almost 1.5 times higher than that of a 194 THz (widely used telecom wavelength) optical communication (20 Mb/s). The performance gap between optical frequencies and RF frequencies reduces further as the communication distance increases as explained in the following section. In this analysis, the R_b is calculated using (2) and the data rate estimation formula given in Section V-A. The estimation of R_b varies significantly with the link budget parameters and modulation formats. In this manuscript, a sample comparative analysis is presented that can be tailored effectively with any given parameter space.

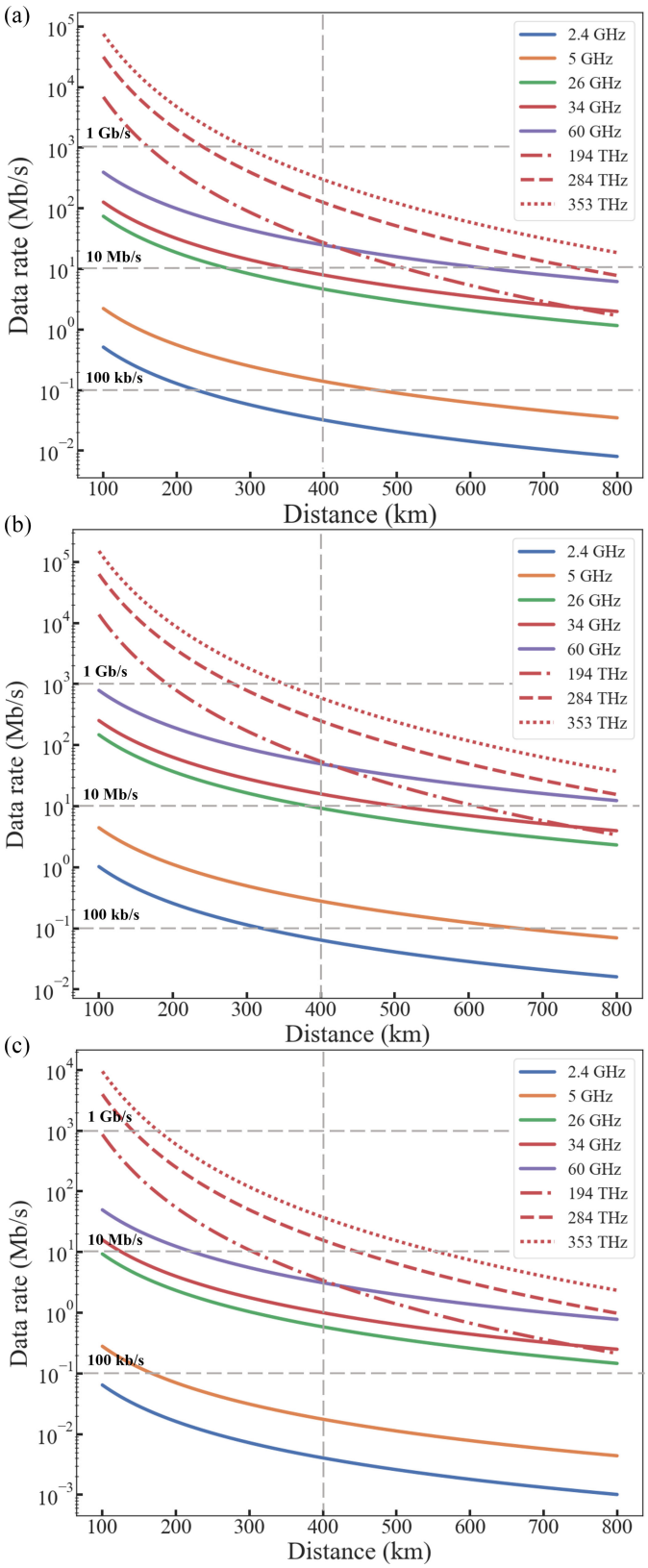

Fig. 7. Example of achievable data rates for different carrier frequencies and modulation formats. (a) OOK. (b) 4-QAM. (c) 2-PPM.

B. Crossover Distance and Crossover Data Rate

The crossover distance r_{cross} is defined as the communication distance at which a microwave (RF and mmWave) communication system demonstrates an equal or better performance than that of a given optical communication system. The crossover data rate R_{Bcross} between a microwave and optical communication system is defined as the data

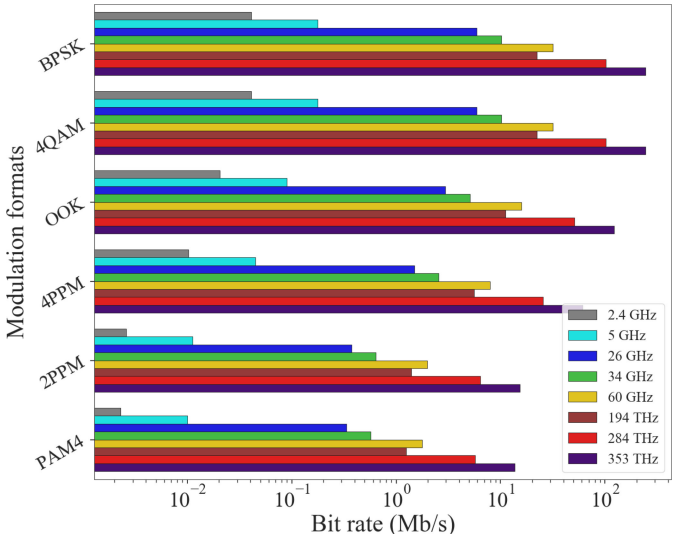

Fig. 8. Example of achievable data rates at 500 km in different modulation formats.

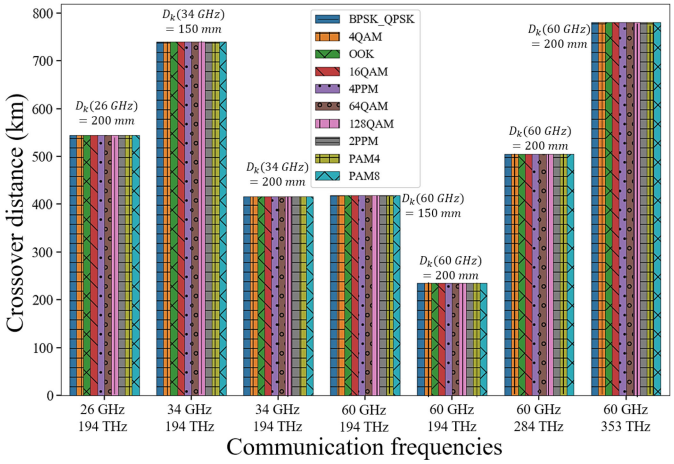

Fig. 9. Crossover distances between microwave and optical communication systems. Five microwave frequencies, three optical frequencies, and ten different modulation schemes are considered to illustrate the r_{cross}. The antenna sizes for the microwave systems are given at the top of each column. The compared operating frequencies are given as the x-axis.

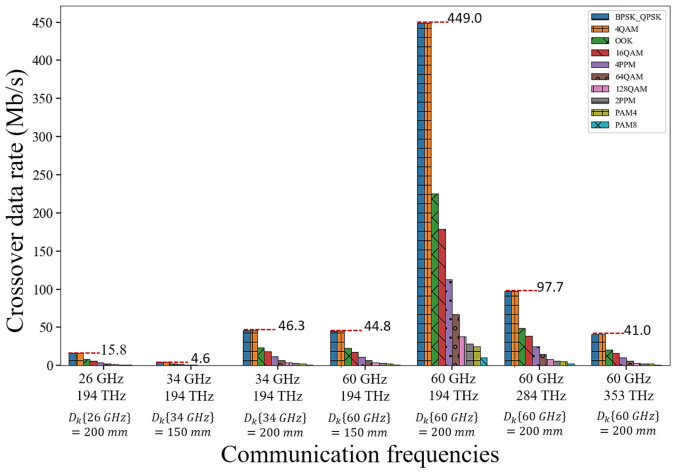

Fig. 10. Data rate at the crossover distance for different communication systems.

rate at the crossover distance, $r = r_{\text{cross}}$. To study and compare the performance crossover in detail, in our sample analysis, we consider microwave communication systems which are selected from the following parameter sets: microwave frequency= {2.4 GHz, 5.0 GHz, 26 GHz, 34 GHz, 60 GHz} and microwave antenna size= {50 mm, 100 mm, 150 mm, 200 mm}. Three optical communication frequencies are considered, optical frequency= {194 THz, 284 THz, 353 THz}. For all sample optical systems, a 10-mm Tx aperture and a 50 mm Rx aperture are considered. Besides, a 1 W transmit power for all communication links and up to 800 km communication distance ($r_{\text{lim}} = 800$ km) are taken into account for the analysis. With the design parameters given in Table II, the sample crossover distances between microwaves and optical channels with different antenna sizes and modulation schemes are calculated (numerically) and presented in Fig. 9. Interestingly, the crossover distance $r_{\text{cross}}(i-j)$ between a microwave system i and optical system j is independent of the modulation schemes. The crossover distance for given design parameters defined as the distance at which both microwave and optical wireless links have equal channel capacities, $C_i(r_{\text{cross}}) = C_j(r_{\text{cross}})$, where C_i and C_j denote the channel capacities of microwave system and optical systems.

We can see from Fig. 9 that between the given 26 GHz (with 200-mm antenna) microwave system and the given 194 THz optical communication system, the performance crossover distance is about 540 km regardless of the modulation formats. However, the crossover distance changes with the system design parameters. For instance, the r_{cross} between 34 GHz (with 200-mm antenna) mmWave system and 194 THz optical is around 416 km that is about 125 km smaller than the previously mentioned r_{cross} between 26 GHz and 194 THz systems. Therefore, the given 26 GHz and 34 GHz microwave systems tend to perform better compared to the considered optical system at distances $r > 540$ km and $r > 416$ km, respectively. Any system pairs S_c other than the presented ones in Fig. 9 do not have r_{cross} within the considered maximum distance (r_{lim}). That is to say, the sample optical systems show a higher data rate than those of RF and mmWave systems which are not mentioned in Fig. 9 for $r \leq r_{\text{lim}}$. On the other hand, the R_{Bcross} of different modulation formats is quite different from each other as each format requires a certain E_b/N_o to achieve a desired BER, as described in (3). Therefore, $R_{\text{Bcross}} = f(E_b/N_o(\textit{modulation formats}))$. As an illustration, the calculated R_{Bcross} for different S_c and modulation formats is presented in Fig. 10. We can see that the crossover data rates between 60 GHz (150-mm antenna) and 194 THz channels are 22.5, 44.8, and 2.8 Mb/s for OOK, 4 QAM, and 2PPM modulation schemes, respectively. The crossover data rate scales with the antenna size and the operating frequencies. It can be seen from Fig. 10 that about ten times higher crossover data rate is possible between a 60 GHz and a 194 THz communication system by increasing the microwave antenna size to 200 mm. The performance crossover distance and performance

crossover data rate between microwave and optical systems are dictated by the system design parameters, e.g., antenna sizes, transmit power, etc. In the above-mentioned study, we provide sample calculations of the possible performance crossovers based on the selected parameters. The analysis can be done with any design parameters set to study and understand the performance reach of the communication technologies.

VI. Summary and Discussion

In this article, we study the achievable performance of the available wireless technologies (RF, mmWave, and optical) to establish omnidirectional CubeSat crosslink. Since each technology possesses its distinct advantages and limitations in the CubeSat platform, we present a comprehensive study of the performance of communication links in terms of design parameters, power consumption, data rate, and modulation formats. Our study shows that the incorporation of the required number of large microwave antennas and PAAs to achieve omnidirectional communication is tremendously challenging in a resource-limited CubeSat platform. As studied in Section IV, the current CubeSats are not capable to deliver the required high power to achieve omnidirectionality in static antenna and PAA-based microwave systems. In contrast, the optical communication system demonstrates the potential to achieve omnidirectional multi-Gb/s data communication due to its low total power consumption and the availability of compact (smaller than 15 mm in diameter), high-speed (in the order of kHz) scanning mirrors. Furthermore, our analyses reveal that although the optical communication demonstrates one to two orders of magnitude higher data rate than the microwave system up to a certain communication distance, at a longer distance (e.g., 400 km and beyond), the mmWave point-to-point communication system (e.g., 60 GHz) has the potential to perform better than the optical system (e.g., 194 THz) in considered CubeSat platform. We show that there exists a performance crossover between microwave and optical communication links due to the tradeoffs among the system design parameters. The performance crossovers between microwave and optical communication links are analyzed in detail to assess the maximum reach and maximum data rate. The right selection of the communication medium in a CubeSat crosslink depends on the application, the integrable antenna size, the available power, the desired data rate, and the desired communication range. The analysis presented in this article can be used as a reference for high-speed omnidirectional CubeSat link development with appropriate design parameters.

Disclosure

The authors declare no conflicts of interest.

References

[1] W. J. Blackwell *et al.*, "Overview of the NASA TROPICS CubeSat constellation mission," in *Proc. CubeSats NanoSats Remote Sens. II*, vol. 10769, 2018, pp. 64 – 73.

[2] S. Corpino and F. Nichele, "CubeSats to support Mars exploration: Three scenarios for valuable planetary science missions," in *Proc. 12th Reinventing Space Conf.*, 2017, pp. 17–32.

[3] J. E. Velazco *et al.*, "Inter-satellite omnidirectional optical communicator for remote sensing," in *Proc. CubeSats NanoSats Remote Sens. II*, vol. 10769, Sep. 2018, Art. no. 107690L.

[4] J. A. Ruiz-de Azua *et al.*, "Proof-of-concept of a federated satellite system between two 6-unit CubeSats for distributed earth observation satellite systems," in *Proc. IEEE Int. Geosci. Remote Sens. Symp. (IGARSS)*, Jul. 2019, pp. 8871–8874.

[5] D. Selva, A. Golkar, O. Korobova, I. L. i. Cruz, P. Collopy, and O. L. de Weck, "Distributed earth satellite systems: What is needed to move forward?" *J. Aerosp. Inf. Syst.*, vol. 14, no. 8, pp. 412–438, 2017. [Online]. Available: https://doi.org/10.2514/1.I010497

[6] Z. T. Lee, "CubeSat constellation implementation and management using differential drag," M.S. thesis, Dept. Aeronaut. Astronaut., Massachusetts Inst. Technol., Cambridge, MA, USA, 2017. [Online]. Available: https://dspace.mit.edu/handle/1721.1/112471

[7] I. U. Zaman, J. E. Velazco, and O. Boyraz, "Realization of omnidirectional CubeSat crosslink by wavelength-selective optical transceiver," *IEEE J. Miniat. Air Space Syst.*, vol. 1, no. 1, pp. 47–55, Jun. 2020.

[8] Y. Kovo. *2.0 Complete Spacecraft Platforms*. Accessed: Mar. 2020. [Online]. Available: http://www.nasa.gov/smallsat-institute/sst-soa-2020/complete-spacecraft-platforms

[9] EnduroSat. *1U CubeSat Platform CubeSat Platforms*. Accessed: Nov. 2020. [Online]. Available: https://www.endurosat.com/cubesat-store/cubesat-platforms/1u-cubesat-platform/

[10] S. Sanchez-Sanjuan, J. Gonzalez-Llorente, and R. Hurtado-Velasco, "Comparison of the incident solar energy and battery storage in a 3U CubeSat satellite for different orientation scenarios," *J. Aerosp. Technol. Manag.*, vol. 8, no. 1, pp. 91–102, Mar. 2016. [Online]. Available: http://www.jatm.com.br/ojs/index.php/jatm/article/view/531

[11] N. M. Suhadis, "Statistical overview of cubesat mission," in *Proc. Int. Conf. Aerosp. Mech. Eng.*, 2020, pp. 563–573.

[12] Y. Kovo. *Power*. Accessed: Mar. 2020. [Online]. Available: http://www.nasa.gov/smallsat-institute/sst-soa-2020/power

[13] EnduraSat. *12U CubeSat Platform CubeSat Platforms*. Accessed: Nov. 2020. [Online]. Available: https://www.endurosat.com/cubesat-store/cubesat-platforms/12u-cubesat-platform/

[14] K. Devaraj *et al.*, "Planet high speed radio: Crossing Gbps from a 3U CubeSat," in *Proc. Small Satellite Conf.*, Aug. 2019, pp. 1–15. [Online]. Available: https://digitalcommons.usu.edu/smallsat/2019/all2019/106

[15] K. Leveque, L. Carleton, J. King, Z. Cuseo, and R. Babb, "Unlocking the next generation of nano-satellite missions with 320 Mbps ka-band downlink: On-orbit results," in *Proc. Small Satellite Conf.*, Aug. 2019, pp. 1–15. [Online]. Available: https://digitalcommons.usu.edu/smallsat/2019/all2019/110

[16] J. E. Velazco *et al.*, "High data rate inter-satellite omnidirectional optical communicator," in *Proc. 32nd Annu. AIAA/USU Conf. Small Satellites*, 2018, p. 2.

[17] R. W. Kingsbury, "Optical communications for small satellites," Ph.D. dissertation, Dept. Aeronaut. Astronaut., Massachusetts Inst. Technol., Cambridge, MA, USA, 2015.

[18] R. Morgan and K. Cahoy, "Nanosatellite lasercom system," in *Proc. 31st Annu. AIAA/USU Conf. Small Satellites*, 2017, pp. 1–32.

[19] I. U. Zaman and O. Boyraz, "Impact of receiver architecture on small satellite optical link in the presence of pointing jitter," *Appl. Opt.*, vol. 59, no. 32, pp. 10177–10184, Nov. 2020. [Online]. Available: http://ao.osa.org/abstract.cfm?URI=ao-59-32-10177

[20] P. Grenfell, A. Aguilar, K. Cahoy, and M. Long, "Pointing, acquisition, and tracking for small satellite laser communications," in *Proc. 32nd Annu. AIAA/USU Conf. Small Satellites*, 2018, pp. 1–7.

[21] C.-C. Chen and C. Gardner, "Impact of random pointing and tracking errors on the design of coherent and incoherent optical intersatellite communication links," *IEEE Trans. Commun.*, vol. C-37, no. 3, pp. 252–260, Mar. 1989.

[22] B. C. Technologies. (2019). *Star Trackers*. [Online]. Available: https://storage.googleapis.com/blue-canyon-tech-news/1/2019/10/BCT_DataSheet_Components_ACS_F2.pdf

[23] J. Chang, C. M. Schieler, K. M. Riesing, J. W. Burnside, K. Aquino, and B. S. Robinson, "Body pointing, acquisition and tracking for small satellite laser communication," in *Proc. Free-Space Laser Commun. XXXI*, vol. 10910, 2019, pp. 144–152. [Online]. Available: https://doi.org/10.1117/12.2511159

[24] I. U. Zaman, J. E. Velazco, and O. Boyraz, "Omnidirectional optical crosslinks for CubeSats: Transmitter optimization," *IEEE Trans. Aerosp. Electron. Syst.*, vol. 56, no. 6, pp. 4556–4566, Dec. 2020.

[25] Optotune. *Dual Axis VCM With Position Feedback2d Beam Steering*. Accessed: Mar. 2020. [Online]. Available: https://www.optotune.com/contact/49-products/beam-steering

[26] M. Technologies. (2017). *Mirrorcle Technologies MEMS Mirrors—Technical Overview*. [Online]. Available: https://www.semanticscholar.org/paper/Mirrorcle-Technologies-MEMS-Mirrors-

[27] G. GomSpace. *GOMspace—12U*. Accessed: Jan. 2021. [Online]. Available: https://gomspace.com/12u.aspx

[28] D. Roddy, *Satellite Communications*, 4th ed. London, U.K.: McGraw-Hill, Feb. 2006.

[29] V. W. S. Chan, "Optical satellite networks," *J. Lightw. Technol.*, vol. 21, no. 11, pp. 2811–2827, Nov. 2003. [Online]. Available: http://jlt.osa.org/abstract.cfm?URI=jlt-21-11-2811

[30] H. R. Anderson, *Fixed Broadband Wireless System Design*. New York, NY, USA: Wiley, 2003, pp. 203–207.

[31] R. D. Straw, *The ARRL Antenna Book*. Newington, CT, USA: Amer. Radio Relay League, 2000, pp. 15–20.

[32] S. Briatore, R. Akhtyamov, and A. Golkar, "Design and flight test results of high speed optical bidirectional link between stratospheric platforms for aerospace applications," in *Proc. Laser Commun. Propagat. Atmosphere Oceans VI*, vol. 10408, Aug. 2017, Art. no. 1040804. [Online]. Available: https://www.spiedigitallibrary.org/conference-proceedings-of-spie/10408/1040804/Design-and-flight-test-results-of-high-speed-optical-bidirectional/10.1117/12.2273808.short

[33] H. Kaushal, V. Jain, and S. Kar, *Acquisition, Tracking, and Pointing*. New Delhi, India: Springer, Jan. 2017.

[34] Y. Kim *et al.*, "Feasibility of mobile cellular communications at millimeter wave frequency," *IEEE J. Sel. Topics Signal Process.*, vol. 10, no. 3, pp. 589–599, Apr. 2016.

[35] M. Jiang, Z. N. Chen, Y. Zhang, W. Hong, and X. Xuan, "Metamaterial-based thin planar lens antenna for spatial beamforming and multibeam massive MIMO," *IEEE Trans. Antennas Propag.*, vol. 65, no. 2, pp. 464–472, Feb. 2017.

[36] J. D. Dunworth *et al.*, "A 28 GHz bulk-CMOS dual-polarization phased-array transceiver with 24 channels for 5G user and basestation equipment," in *Proc. IEEE Int. Solid-State Circuits Conf. (ISSCC)*, 2018, pp. 70–72.

[37] B. Sadhu *et al.*, "7.2 a 28GHz 32-element phased-array transceiver IC with concurrent dual polarized beams and 1.4 degree beam-steering resolution for 5G communication," in *Proc. IEEE Int. Solid-State Circuits Conf. (ISSCC)*, Feb. 2017, pp. 128–129.

[38] Optotune. (2018). *Dual Axis VCM With Position Feedback*. [Online]. Available: https://www.optotune.com/products/beam-steering/2d-mirror-mr-15-30

[39] I. U. Zaman, A. W. Janzen, R. Torun, M. Peng, J. E. Velazco, and O. Boyraz, "Omnidirectional optical transceiver design techniques for multi-frequency full duplex CubeSat data communication," in *Proc. SPIE Opt. Photon. CubeSats NanoSats Remote Sens. II*, Aug. 2018, pp. 10769–10842.

[40] Analog Devices. *ADL5606 Datasheet and Product Info—Analog Devices*. Accessed: May 2020. [Online]. Available: https://www.analog.com/en/products/adl5606.html

[41] Analog Devices. *HMC751 Datasheet and Product Info—Analog Devices*. Accessed: May 2020. [Online]. Available: https://www.analog.com/en/products/hmc751.html

[42] Analog Devices. *HMC962 Datasheet and Product Info—Analog Devices*. Accessed: May 2020. [Online]. Available: https://www.analog.com/en/products/hmc962.html#product-overview

[43] Analog Devices. *AD9371 Datasheet and Product Info—Analog Devices*. Accessed: May 2020. [Online]. Available: https://www.analog.com/en/products/ad9371.html

[44] DiCon Fiberoptics Inc.. *MEMS Single-Mode 1xN Optical Switches—DiCon Fiberoptics*. Accessed: Jun. 2020. [Online]. Available: https://www.diconfiberoptics.com/products/mems_1_x_n_optical_switches_single_mode.php

[45] Thorlabs. *Lithium Niobate Electro-Optic Modulators, Fiber-Coupled*. Accessed: Jun. 2020. [Online]. Available: https://www.thorlabs.com/newgrouppage9.cfm?objectgroup_id=3918

[46] B. Hall and W. Taylor. *Small Form Factor SATCOM Solutions—Analog Devices*. Accessed: Apr. 2020. [Online]. Available: https://www.analog.com/en/technical-articles/small-form-factor-satcom-solutions.html

[47] B. Yang, Z. Yu, J. Lan, R. Zhang, J. Zhou, and W. Hong, "Digital beamforming-based massive MIMO transceiver for 5G millimeter-wave communications," *IEEE Trans. Microw. Theory Techn.*, vol. 66, no. 7, pp. 3403–3418, Jul. 2018.

[48] I. U. Zaman, A. W. Janzen, R. Torun, J. E. Velazco, and O. Boyraz, "Design tradeoffs and challenges of omnidirectional optical antenna for high speed, long range inter CubeSat data communication," in *Proc. Small Satellite Conf. Delivering Mission Success*, Aug. 2018, p. 6.

[49] M. Toyoshima, "Trends in satellite communications and the role of optical free-space communications [invited]," *J. Opt. Netw.*, vol. 4, no. 6, pp. 300–311, Jun. 2005.

[50] R. S. Fuhrman, "Intersatellite link design issues," Ph.D. dissertation, Telecommun., Univ. Colorado Denver, Denver, CO, USA, 1985.

[51] S. K. Podilchak *et al.*, "Compact antenna for microsatellite using folded shorted patches and an integrated feeding network," in *Proc. 6th Eur. Conf. Antennas Propag. (EUCAP)*, Mar. 2012, pp. 1819–1823.

[52] B. Maamar and X. Mai, "Study and analysis of optical intersatellite links," *Int. J. Electron. Commun. Eng.*, vol. 10, no. 6, p. 5, 2016.

[53] "TM synchronization and channel coding summary of concept and rationale," Consult. Committee Space Data Syst., Washington, DC, USA, Rep. CCSDS 130.1-G-3, Jun. 2020.

[54] *G.709.2: OTU4 Long-Reach Interface*, Int. Telecommun. Union, Geneva, Switzerland, Jul. 2018.

[55] A. Goldsmith, *Wireless Communications*. Cambridge, U.K.: Cambridge Univ. Press, 2005, pp. 171–176.

[56] T. Y. Elganimi, "Performance comparison between OOK, PPM and PAM modulation schemes for free space optical (FSO) communication systems: Analytical study," *Int. J. Comput. Appl.*, vol. 79, no. 11, pp. 22–27, Oct. 2013.

[57] S. Trisno, "Design and analysis of advanced free space optical communication systems," Ph.D. dissertation, Elect. Eng., Univ. Maryland, College Park, MD, USA, 2006.